Available online at www.CivileJournal.org

Civil Engineering Journal

(E-ISSN: 2476-3055; ISSN: 2676-6957)

Vol. 12, No. 06, June, 2026

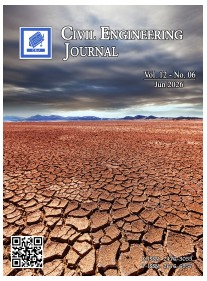

Seismic Microzonation and Site Characterization Along an Active Fault Segment Using Microtremor and Geotechnical Data

Rusnardi Rahmat Putra [1*], Junji Kiyono [2], Sai K. Vanapalli [3], Zhenghu Zhang [4], M. Darma Agung [1], Nurhasan Syah [1], Totoh Andayono [1], Fitra Rifwan [1], Dezy Saputra [1], Ali Basrah Pulungan [5]

[1] *Department of Civil Engineering, Universitas Negeri Padang, Sumatera Barat 25131, Indonesia.*

[2] *Department of Urban Management, Graduate School, Kyoto University, Kyoto, Japan.*

[3] *Department of Civil Engineering, University of Ottawa, Ottawa, ON K1N 6N5, Canada.*

[4] *State Key Laboratory of Coastal and Offshore Engineering, School of Infrastructure Engineering, Dalian University of Technology, Dalian 116024, China.*

[5] *Department of Electrical Engineering, Universitas Negeri Padang, Sumatera Barat 25131, Indonesia.*

Received 27 March 2025; Revised 11 May 2026; Accepted 14 May 2026; Published 01 June 2026

Abstract

The Sianok Segment, one of 19 sections of the Great Sumatran Fault (GSF), extends for 90 km with a minimum slip rate of 14.5 ± 0.5 mm/yr (Bradley et al., 2017). It cuts through densely populated regions of West Sumatra, including Agam Regency, Bukittinggi, Padang Panjang, and Solok, which are highly prone to earthquakes. This study investigates site characteristics and develops a seismic microzonation to assess potential hazards along the Sianok Segment. Data were collected from 45 randomly distributed microtremor recording sites and 10 subsurface investigations (Standard Penetration Test and Cone Penetration Test). Results indicate that predominant periods range from 0.14–1 s in mountainous terrain and exceed 1 s in urban areas such as Padang Panjang, Solok, Pasaman, and Bukittinggi. Regarding liquefaction, the seismic vulnerability index and ground shear strain suggest that most of the region is susceptible to surface cracking ($\gamma > 10^{-3}$) and moderate liquefaction. More severe liquefaction is expected in the flat southeastern zone toward Solok during a major earthquake (0.6 g). The seismic vulnerability index varies with soil resonance frequency and amplification from bedrock to surface, with Bukittinggi and Padang Panjang identified as highly vulnerable. These findings provide essential input for shaking maps, hazard map updates, and disaster mitigation planning along the Sianok Segment.

Keywords: Microtremor Single Observation; Sianok Segment; Liquefaction Potential; Ground Investigation; Ground Motion.

1. Introduction

The Sianok Segment, one of 19 sections of the Great Sumatran Fault (GSF), extends 90 km with a minimum slip rate of 14.5 ± 0.5 mm/yr [1]. It crosses densely populated areas of West Sumatra, including Agam, Bukittinggi, Padang Panjang, and Solok, which are highly vulnerable to earthquakes. Indonesia is situated at the confluence of three major tectonic plates: the Eurasian, Pacific, and Indian Ocean Plates. The Indo-Australian Plate moves northward at 7 mm/yr in the west, while the Pacific Plate shifts at 12 mm/yr in the east [1], making the country highly prone to earthquakes.

* Corresponding author: rusnardi.rahmat@ft.unp.ac.id

https://doi.org/10.28991/CEJ-2026-012-06-08

Indonesia experiences more than 1,200 earthquakes annually with magnitudes exceeding 4.0 on the Richter scale [2]. Sumatra, one of the nation's largest islands, was shaped by tectonic activity associated with the oblique subduction zone, the Mentawai Thrust Fault, and the Great Sumatran Fault Zone [3]. Earthquakes along the Sumatran Fault are typically moderate to strong and shallow, occurring at depths less than 20 km. Such shallow events can cause severe damage and frequently trigger landslides, increasing the region's vulnerability to earthquake-related losses. In western Sumatra, a 500 km fault line extends from Singkarak through Padang Panjang and Padang to Painan [4, 5].

West Sumatra, located on the western coast of Indonesia, is exposed to two major earthquake sources capable of generating large earthquakes and tsunamis. On land, an active fault line traverses Singkarak, Padang Panjang, Padang, and Painan. Earthquake data from 1779–2023 (Figure 1(a)) indicate that the seismic events tend to be shallow with significant magnitudes, such as those recorded in 1928 (Mw 8.4), 1933 (Mw 9.3), 1981 (Mw 8.1), and 2007 (Mw 8.4). West Sumatra also has the potential for tsunamis because it has an earthquake source at sea (subduction) where the Indo-Australian Plate pushes the stable Indonesian plate; a push that exceeds the elasticity of the stable plate will cause large tsunamis, such as those that occurred in 1833 (Mw 9.2), 2005 (Mw 9.3), and 2010 (in Mentawai) [6].

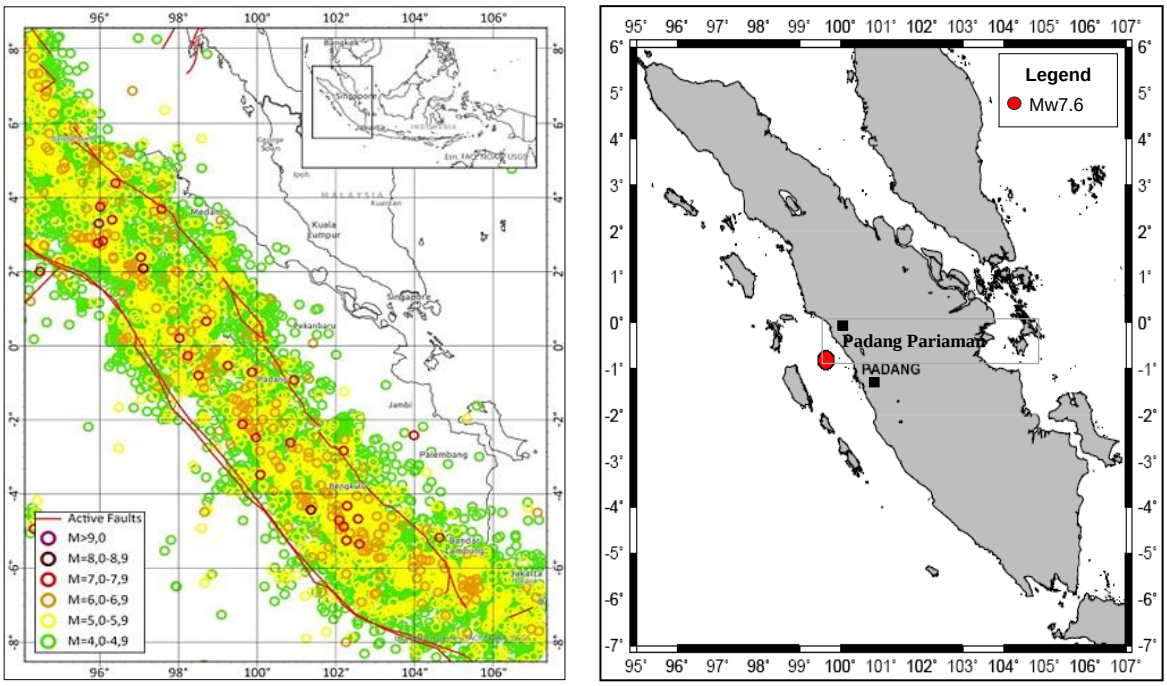

(a) (b)

Figure 1. Seismicity map of Sumatera Island (a) for earthquakes of Mw > 4 from 1779 to 2023 and (b) the latest earthquake of Mw7.6 in 2009

Important insights were gained from the 2009 Padang earthquake, which struck southwest of Pariaman, West Sumatra, with a magnitude of 7.9 and a depth of 71 km. This disaster was a national disaster for the Indonesian state because the number of victims and the earthquake's effect on buildings were extraordinary in West Sumatra and the city of Padang, which is the provincial capital; areas such as Pariaman, Padang Pariaman District, South Pesisir District, West Pasaman, and a small part of Agam Regency were affected.

Based on data from the local government, the earthquake that occurred in West Sumatra on September 30, 2009, caused more significant environmental damage than other natural disasters. Several events occurred during the quake, including building damage, fires, road access being cut off, and landslides.

Figure 2 presents a comparative response spectrum between the specific Padang earthquake and the prevailing Indonesian standard (SNI2002). The peak acceleration necessary for structural design exceeds that stipulated by the Indonesian code at lower levels period, in examples of the damage caused by the earthquake located in Padang Pariaman [7]. The Sianok Canyon is part of a fault that separates Sumatra into two longitudinal parts (the Clover Fault). This fault forms a steep, sometimes perpendicular wall and a green valley fed by the clear water of Batang Sianok. The fault produced a fertile area with a beautiful landscape. Sianok Canyon was formed due to geological processes within the Earth (endogenous) and on its surface (exogenous); specifically, it was formed by folds, faults, and rivers. Through horizontal shift movements of 2 mm/day [7] over thousands of years, a wide gap was formed in Sianok Canyon. The resulting landscape contains a valley and a vast towering cliff.

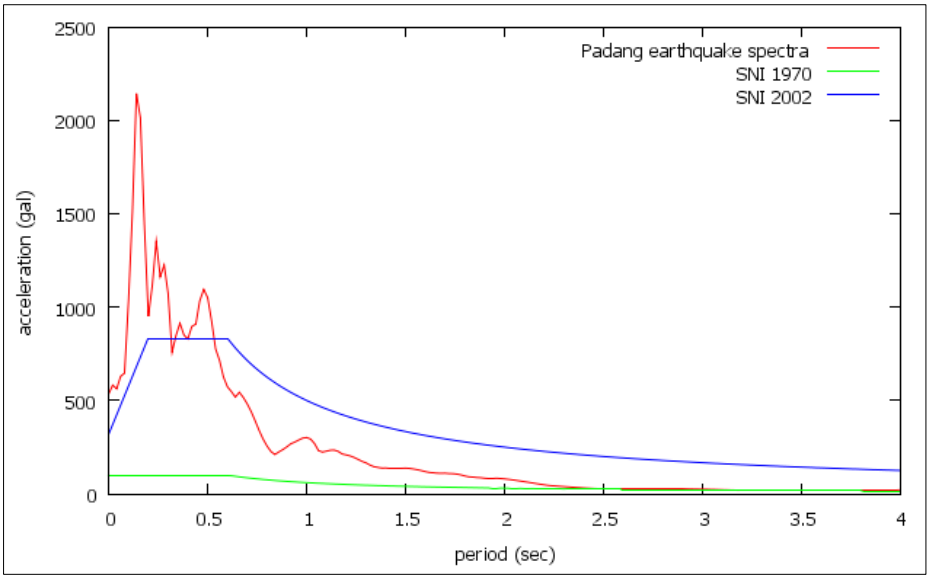

Figure 2. Damage caused by the earthquake: A Comparison of response spectra between the actual Padang earthquake and the existing Indonesian code. (SNI 2002) for rock site condition

The Sianok segment is a densely populated area in West Sumatra that has experienced several destructive earthquakes. Notably, three major events occurred in 1926 and two in 2007, with magnitudes of Mw 6.2, 6.6, and 6.7, respectively. The Sianok segment is also closely associated with volcanic activity. According to the geological map of Lembar Padang, the Great Sumatran Fault (GSF) extends from 100°09′30″E and 0°00′ at the northern foot of Bukit Batan Tinjaulaut to the southwestern flank of Mount Marapi (100°25′00″E and 0°24′30″S), near Kotobaru village [8]. The fault continues near Paninjauan (100°26′30″E and 0°27′15″S), merging with the Sumpur River Valley and extending through the eastern wall of Lake Singkarak. Several secondary faults run parallel to or at an angle of ±30° relative to the main trace. The Sianok fault is classified as active, as it dissects Quaternary alluvial deposits (Qal) in southern Malalu near Bonjol [9].

Geodetic studies report a slip rate of 13.7 ± 1.6 mm/year along this fault [10], consistent with earlier estimates of approximately 14 mm/year [11]. Given these tectonic characteristics, local site effects and geological variability play a critical role in controlling ground motion, structural damage, and financial losses. The Sianok segment extends from the eastern margin of Lake Singkarak, passes the southwestern slope of Mount Marapi, and continues to the Sianok Canyon, spanning a length of about 90 km. Its maximum potential earthquake magnitude has been estimated at Mw 7.3 [12]. The strongest historical event was recorded on August 4, 1926, with the epicentral region located between Bukittinggi and Lake Singkarak. More recently, damaging earthquakes occurred on March 6, 2007 (Mw 6.3 and Mw 6.4), affecting Batu Sangkar and Solok, and on April 8, 2023 (Mw 4.5), which triggered a landslide at Ngarai Sianok in Bukittinggi [12, 13].

In Indonesia, earthquake-resistant building codes consider national-scale seismic hazard maps that integrate fault distributions and bedrock conditions [14, 15]. However, these national maps cannot fully capture the influence of local geological conditions, which strongly control site response. Therefore, detailed seismic microzonation based on field investigations is essential to support safe urban planning and disaster mitigation [16, 17]. Among available methods, the horizontal-to-vertical spectral ratio (HVSR) technique using microtremor data has been widely applied to estimate site-specific resonance frequencies and amplification factors. Previous studies in Indonesia have successfully employed microtremor observations to characterize soil conditions in Padang [18], Palu [19], and more recently in Bukittinggi and Padang Panjang, which lie along the Sianok Segment [20, 21]. These works confirm the presence of soft volcanic and alluvial deposits with low shear-wave velocities (Vs < 200 m/s), leading to significant amplification of ground motion during earthquakes.

In addition to geophysical approaches, geotechnical investigations such as Cone Penetration Tests (CPT) and Standard Penetration Tests (SPT) have been widely used in West Sumatra to directly evaluate subsurface soil characteristics. CPT results provide continuous depth profiles of tip resistance (qc), sleeve friction (fs), and pore pressure (u_2), which are essential for classifying soil layers, estimating relative density, and evaluating liquefaction potential [22, 23]. When combined with HVSR data, CPT measurements allow for the calibration of shear-wave velocity (Vs) models and the validation of resonance frequencies derived from ambient vibration analyses. Several studies have shown that integrated CPT–HVSR investigations yield more reliable seismic microzonation maps because they link dynamic site response parameters (f_0 , A_0 , Kg) with static soil indices (qc, fs, NSPT) [24, 25]. Recently, Setiawan et al. (2024) demonstrated that integrating q-CPT data with HVSR inversion can significantly improve subsurface Vs profiles, highlighting the effectiveness of such hybrid approaches for seismic site characterization [26].

Very recent studies across Indonesia also confirm the growing use of HVSR for soil characterization. Zaenudin et al. (2024) [27] produced two-dimensional shear-wave velocity models beneath Bandar Lampung using HVSR inversion; Prasetya et al. (2024) [28] applied HVSR to assess seismic vulnerability at the Yogyakarta International Airport underpass; Susilo et al. (2025) [29] conducted HVSR inversion in Malang Regency for site characterization; Amelia et al. (2025) [30] analyzed HVSR microtremors in Quaternary sediments of Takalar Regency; and Yulianto (2025) [20] applied HVSR for preliminary site classification in the western Bandung Basin. These recent contributions demonstrate the rapid advancement of HVSR applications in Indonesia, yet none have focused on the Sianok segment, nor have they systematically integrated HVSR with CPT/SPT geotechnical data.

Despite these advances, most existing research in the Sianok corridor has been limited to mapping fundamental frequencies (f_0) and qualitative amplification (A_0). Few studies have advanced toward quantitative shear-wave velocity (Vs) profiling, amplitude reliability assessment, or the consideration of 2D/3D basin and canyon effects (e.g., Ngarai Sianok). Furthermore, the integration of CPT or SPT datasets with HVSR analyses remains scarce, even though such an approach can significantly improve the accuracy of local seismic hazard assessment. Addressing these gaps by combining geotechnical CPT investigations with HVSR observations will provide a more robust characterization of soil conditions and seismic hazard in the Bukittinggi–Padang Panjang region (see Figure 3).

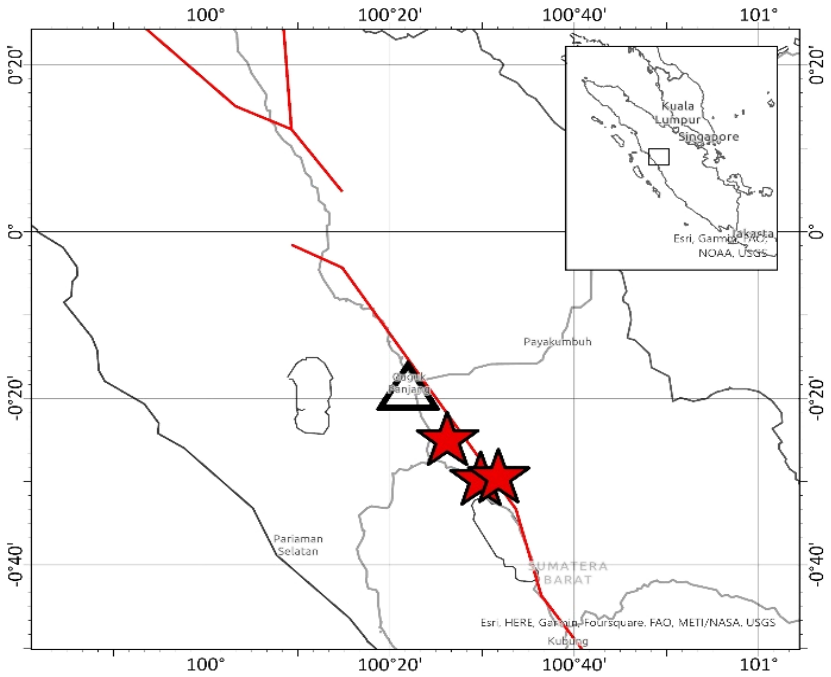

Figure 3. Earthquake events occurred along the Sianok fault; the red stars indicate the earthquake site, the red stars indicate the earthquake event sites, and the triangle is the installed accelerometer site

This study aims to provide surface geological characteristics and vulnerability micro zoning as one of the components of the assessment of earthquake disasters in the Sianok Fault area. This microtremor recording is intended to determine the characteristics of soil dynamics as a basis for preparing micro zoning maps of earthquake shock hazards in the study area. The results of this research are also expected to be used as an essential reference in regional spatial planning.

2. Material and Methods

In addition to the earthquake mechanism, the site characteristics of each installed sensor are collected. The earthquake data is then screened using the fast Fourier transform (FFT) method [31-34] before being plotted based on the site characteristics. Microtremors are exceedingly minute ground vibrations that can be documented at ground level. They may be induced by a variety of stimuli, such as wind, traffic, or ocean waves. Microtremor recordings can be described using one vertical and two horizontal components. This study collected data using the GPL-6A3P microtremor device. First, the horizontal-to-vertical spectral ratio (HVSR) is calculated for each location. The peak period of the HVSR is known to correspond to the site's resonance period, which is calculated using a form of the Fourier spectrum. The study successfully carried out 43 site surveys (Figure 4), taking samples along the Sianok Fault. The research procedure is outlined in Figure 5.

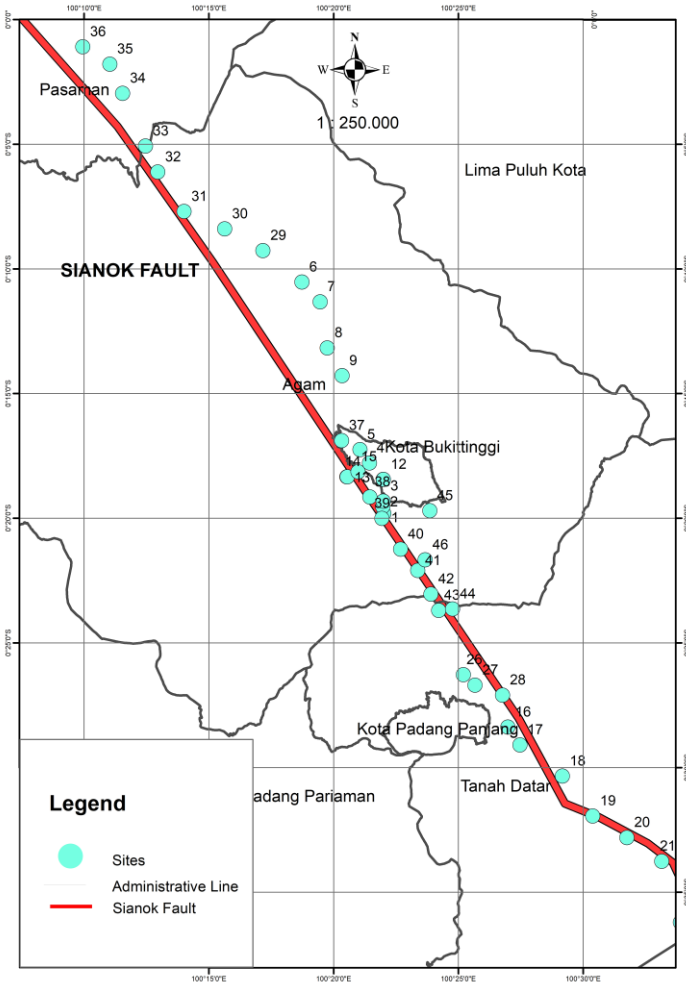

Figure 4. Distribution of microtremor recording sample points in the study area

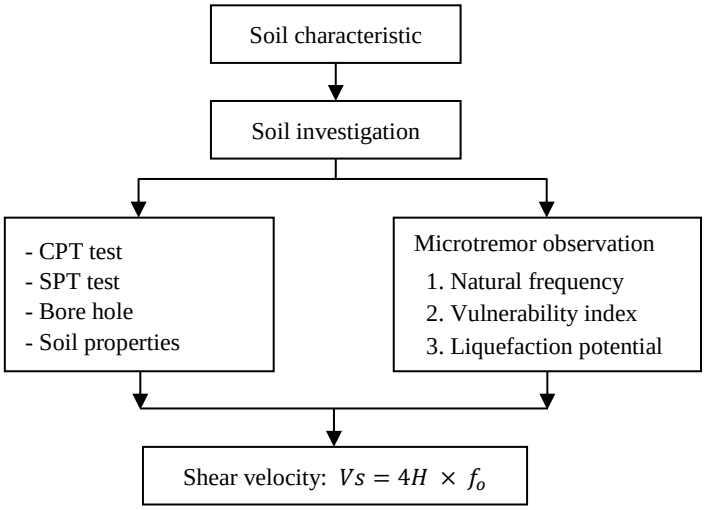

Figure 5. Research procedures

This study successfully performed 43 site surveys (Figure 4) in which samples were taken along the Sianok Fault. The research procedure is outlined as depicted in Figure 5.

Equation 1 presents the formula utilised for calculating the HVSR based on the recorded data

$$HVSR = \sqrt{\frac{F_{NSi}(\omega)^2 + F_{FWi}(\omega)^2}{F_{UDi}(\omega)^2}} \quad (1)$$

where, $F_{NSi}(\omega)$ and $F_{UDi}(\omega)$ are the Fourier amplitude of the NS, EW. UD is the components of each interval, respectively, and ω is the frequency.

The horizontal (comprising North-South and East-West orientations) and vertical (Up-Down) components were simultaneously recorded over a period of ten minutes at a sampling frequency of 100 Hz. This process was divided into 10 segments of 10 seconds each, in accordance with the guidelines outlined in Susilo et al. [29] and Nakamura [35]. Microtremor measurement utilising spectral ratios is regarded as the most dependable and uncomplicated method for assessing the soil structure and dynamic attributes, including the natural frequency of the soil. The HVSR method proposed by Nakamura [36] and Nakamura [37] has been widely used in other studies [38, 39]. This method helps estimate local seismic ground responses. Estimates of the HVSR ground frequency and peak amplitude solely reflect the fundamental soil site frequency and amplification factors in the absence of seismic activity, as discussed in Natawidjaja [40] and Natawidjaja & Triyoso [41]. Comprehensive microtremor recordings can be obtained from both vertical and horizontal components [42].

The non-destructive HVSR microtremor method has become a popular method many researchers use to conduct studies of simple and rapid seismic responses. Geophysical in-situ investigations necessitate distance profiles that often extend over several tens of meters, which can be challenging to obtain at certain sites—such as historical monuments, slopes, hills, or buildings—due to spatial limitations. However, microtremor measurements offer a viable solution to this issue.

3. Results and Discussion

3.1. Microtremor Measurement and Predominant Period

This study used 45 microtremor recording data points scattered randomly along the Sianok Fault. Clear peak waves in the HVSR from the observed sites are correlated with the predominant period conditions and local geology, i.e., the shear wave velocity and sediment thickness [43-45] Figure 6 shows an example of an HVSR plot with a clear peak. Given that T = 1/f, where T is the predominant period and f is the frequency, the relationship between the predominant period based on microtremor recordings [45] and the soil classification can be seen in Table 1.

Table 1. HVRs result along Sianok fault

Site	Lat	Long	Fo (Hz)	T(s)	Site	Lat	Long	Fo (Hz)	T(s)
1	-0.33	100.4	2.77	0.36	24	-0.68	100.6	0.21	4.81
2	-0.33	100.4	2.52	0.40	25	-0.44	100.4	2.65	0.38
3	-0.32	100.4	1.31	0.77	26	-0.44	100.4	2.55	0.39
4	-0.30	100.4	3.21	0.31	27	-0.45	100.4	0.36	2.79
5	-0.29	100.4	3.56	0.28	28	-0.15	100.3	0.28	3.55
6	-0.18	100.3	1.45	0.69	29	-0.14	100.3	0.53	1.89
7	-0.19	100.3	2.08	0.48	30	-0.13	100.2	0.25	4.05
8	-0.22	100.3	5.79	0.17	31	-0.10	100.2	0.33	3.01
9	-0.24	100.3	2.80	0.36	32	-0.08	100.2	0.34	2.91
10	-0.31	100.4	2.46	0.41	33	-0.05	100.2	0.19	5.18
11	-0.31	100.4	0.93	1.07	34	-0.03	100.2	0.20	5.09
12	-0.31	100.3	2.14	0.47	35	-0.02	100.2	0.24	4.19
13	-0.31	100.3	1.70	0.59	36	-0.28	100.3	0.76	1.31
14	-0.30	100.3	2.54	0.39	37	-0.32	100.4	0.40	2.51
15	-0.47	100.4	0.20	5.05	38	-0.33	100.4	1.38	0.73
16	-0.48	100.5	0.24	4.10	39	-0.35	100.4	1.98	0.50
17	-0.51	100.5	0.32	3.16	40	-0.37	100.4	7.34	0.14
18	-0.53	100.5	0.24	4.16	41	-0.38	100.4	2.91	0.34
19	-0.55	100.5	0.34	2.91	42	-0.40	100.4	6.10	0.16
20	-0.56	100.6	0.21	4.88	43	-0.39	100.4	2.93	0.34
21	-0.60	100.6	0.24	4.10	44	-0.33	100.4	0.20	5.03
22	-0.61	100.6	0.24	4.09	45	-0.36	100.4	1.45	0.69
23	-0.65	100.6	0.21	4.87					

Based on microtremor observations and HVSR analysis (Figure 6), a map illustrating the predominant period for the Sianok Fault was generated utilising spatial interpolation techniques method. Based on the predominant frequency map (Figure 7), it is evident that there exists a significant correlation between the predominant frequency of the foundational soil and the characteristics of the local environment site; high predominant period values (>1s) are observed in soft sediments in the southeastern zone of Tanah Datar Regency towards Solok Regency and the border zone between Agam Regency and Pasaman Regency. In contrast, thicker sediments above the bedrock with low periods were observed in the Agam Regency Zone and Bukittinggi (Table 1). Based on the dominant period analysis results, the area around the Sianok Fault has a dominant period in the range of 0.14–5.12 s. The result obtained from the current study is suitable with the result proposed by Ansal et al. [1]. Soil predominance maps offer significant insights for evaluating soil structural resonance in areas at potential risk, utilising the correlation between foundational building frequencies and the heights of reinforced structures [46, 47]. Commonly, existing buildings are 1-3 stories, and houses are non-engineered structures.

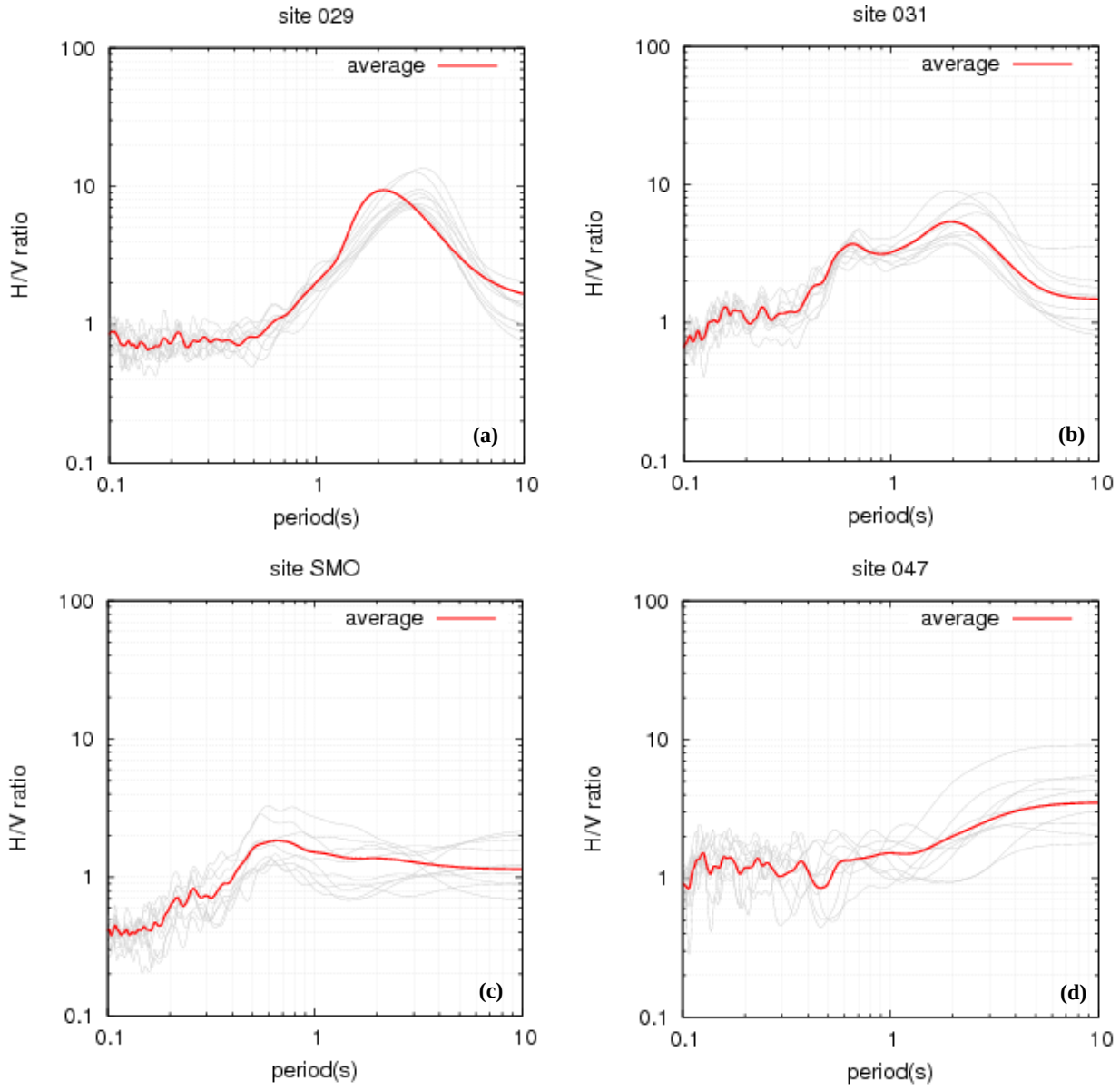

Figure 6. Example of HVSRs (the red line represents the average, and the black line denotes the sampled HVSR). (a) Peak exceeding 1 s; (b) HVSR exhibits two peaks; (c) Peak less than 1 s; (d) No discernible peak

In Figure 7 Natural frequency and period from microtremor observation results, (a) Frequency-based cross-sectional profile along horizontal direction site 1-45 of the study area and (b) map of natural period along of Sianok segment. The frequency of sediment deposits at Pasaman in the north, Padang Panjang, and Tanah Datar in the south are relatively similar, being less than 1 Hz (natural period 1s), except for some parts of Bukittinggi, which have a frequency greater

than 1 Hz (natural period <1s) (Figures 6-a and 6-b). The natural period indicates soil characteristics at the surface <1s (short period) correspondence to soft and > 1s (long period) to rock. The low frequencies (<1 Hz) in Pasaman indicate deep soft sediments and prone to long-period amplification affecting tall buildings and infrastructure. The mid frequencies (2–4 Hz) in Agam suggest moderate sediment thickness may amplify ground motion affecting 2–4 story buildings. The higher fluctuations (2–6 Hz) in Padang Panjang–Tanah Datar imply complex site response with both volcanic slopes and valley fills risk of localized amplification and potential landslide resonance.

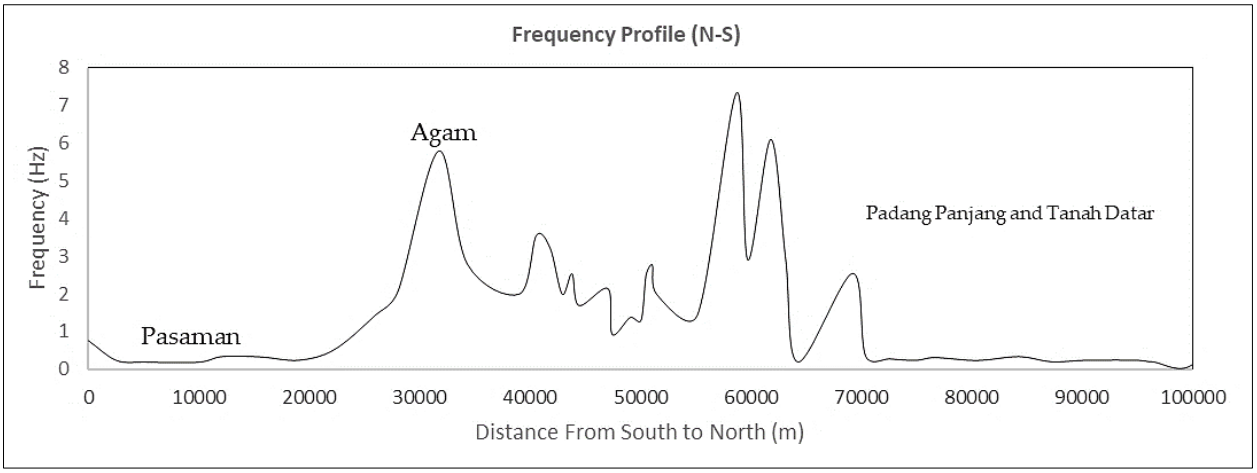

(a)

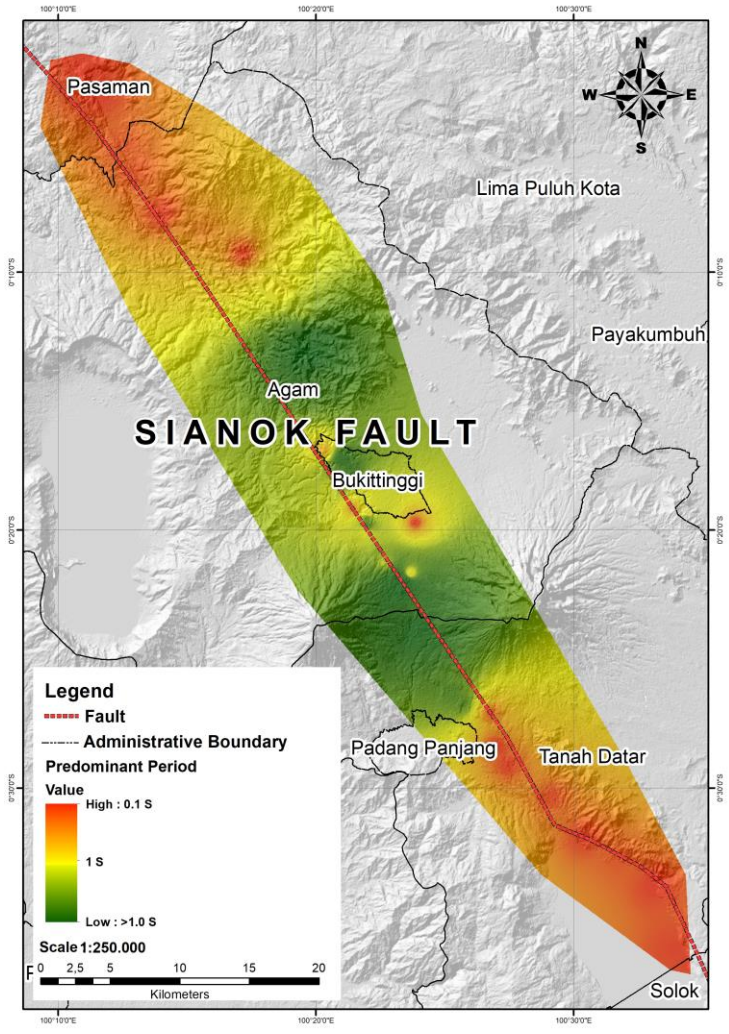

(b)

Figure 7. Natural frequency and period from microtremor observation results, (a) Frequency-based cross-sectional profile along horizontal direction site 1-45 of the study area and (b) map of natural period along of Sianok segment

3.2. Sediment Thickness

Regarding the H/V Ratio and sediment thickness, multiple research studies [48-50] demonstrate that microtremor measurements can be employed to ascertain the surface sediment thickness. Quantitative correlations between this thickness and the fundamental frequency of the sediment, as identified through the peak of the H/V spectral ratio of microtremors [36], the predominant rocks surrounding the Sianok segments are relatively recent volcanic rocks from the Quaternary period, followed by rocks from the Tertiary and Permian periods [51, 52] have shear velocity ranges from 700 to 3000 m/s. Based on the geology data and natural frequency from microtremor observation results along the Sianok segment, We determine the depth of the initial stratum within the subsurface architecture through a systematic analysis.

$$Vs = 4H \times f_o \quad (2)$$

where the *Vs* is the shear velocity, *H* is the first layer depth and *fo* is the natural frequency of the first layer. There are approximately 10 soil investigation points installed along the Sianok segment. Each sensor is distributed and installed along the segment based on practicality and ease of installation (Figure 6-b). From these soil investigations, the soil characteristics of the first layer can be determined. Geospatial interpolation is performed to determine the depth of the first layer along the Sianok segment. The first layer at each site is identified at depths ranging from 7.5 to 10.5 meters (Figure 6-c).

The fault trace (red dashed line in the legend) runs NW–SE, parallel to the long axis of Sumatra—typical for the right-lateral strike-slip GSF. Near Bukittinggi, the trace coincides with a linear valley (the Sianok canyon area). Linear valleys, aligned ridges, and sudden drainage bends are classic surface expressions of a strike-slip fault. Around Padang Panjang and toward Tanah Datar, you see a star-burst hill pattern—that's the morphologic signature of a volcanic cone (Marapi) superimposed on the fault zone. The fault skirts these volcanic slopes; local releasing or restraining bends may occur where the line deviates. How to read terrain classes geotechnically (typical, site-effect oriented view) Valleys & Flat plains (dark green/yellow): Usually young, soft sediments (alluvium, colluvium, lake deposits) (Figure 8).

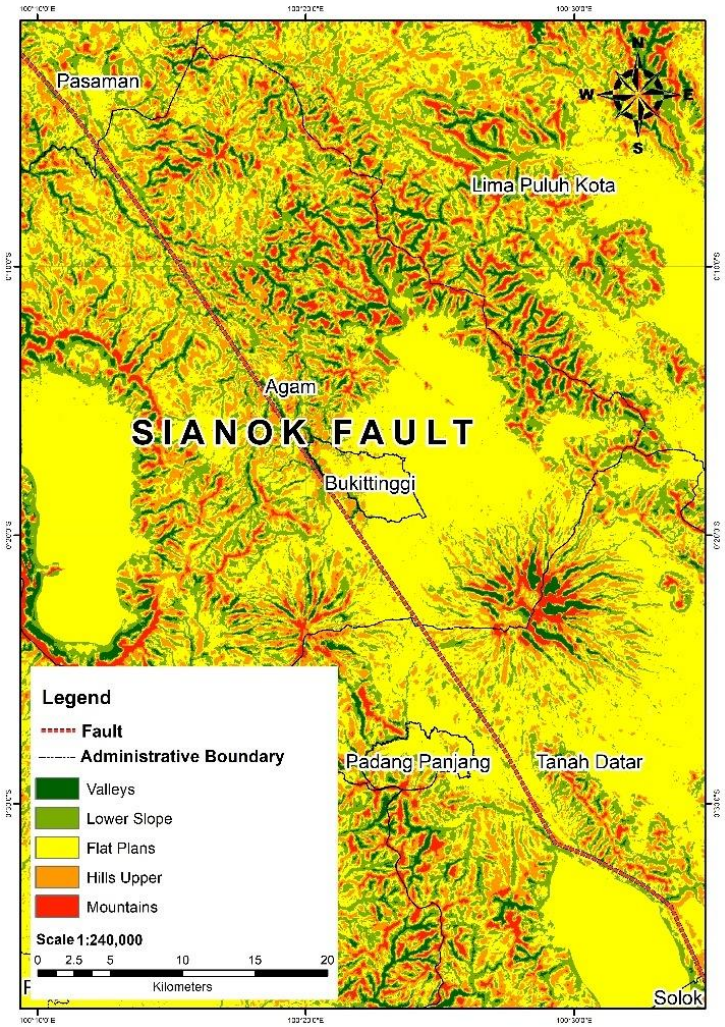

Figure 8. Land use maps along Sianok segment

Figure 9-b shows the average depth of topsoil (the first layer) is 7.5-10 m, and Figure 9-c shows that the shear velocity at the surface of the Sianok Segment is 0-150 m/s in the south-east area (Solok, Tanah Datar, and some parts in Padang Panjang areas), Bukittinggi, and Nort-West (Pasaman) and is greater 150 m/s in the middle of the Sianok segment (Agam).

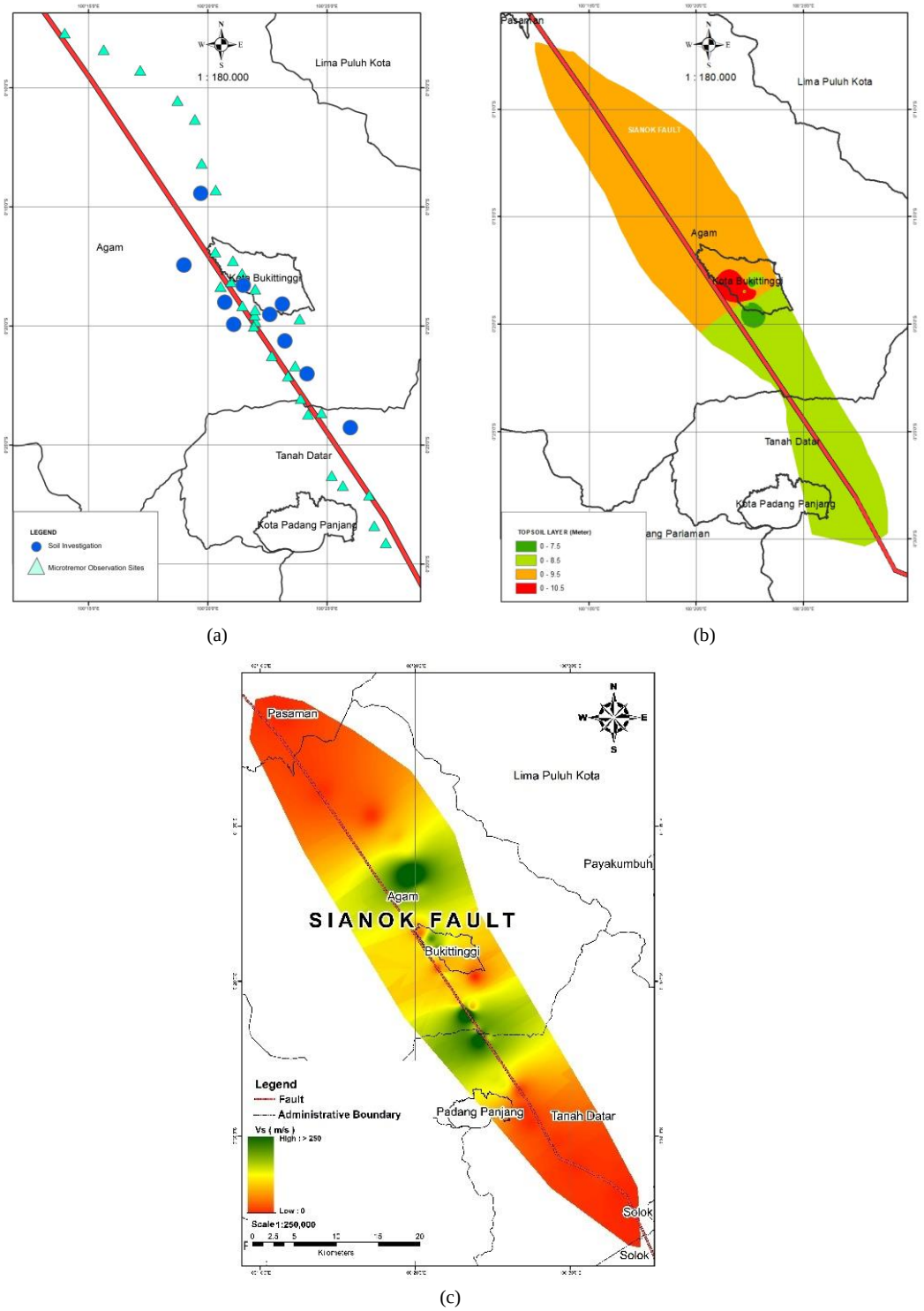

Figure 9. (a) installed soil investigation sites, blue circles are soil investigation sites, and cyan blue triangles are microtremor observation sites, (b) topsoil layer depth, (c) shear velocity of the top layer.

3.3. Seismic Vulnerability Index

The seismic vulnerability index indicates the level of susceptibility of the superficial soil layer to deformation during seismic events. This index helps identify relatively weak areas during an earthquake. It is important to consider the region's geological conditions when assessing the seismic vulnerability index for a location.

The natural frequency and amplification values derived from the microtremor spectrum analysis significantly influence the seismic vulnerability index. Elevated levels of this index are typically observed in regions characterised by a low resonance frequency. Putra et al. [47] has shown a clear link between the seismic vulnerability index (Kg) and the level of earthquake-induced damage. The seismic vulnerability index is calculated by squaring the maximum value of the microtremor spectrum and dividing it by the resonant frequency, as outlined in Nakamura [37].

$$K_g = \frac{A^2}{f_0} \tag{3}$$

where A represents the amplification factor and f_0 denotes the natural frequency of the soil in the area under consideration studied.

Figure 10 depicts a map illustrating the seismic vulnerability index for the Sianok Fault region. The image presents various seismic vulnerability values pertinent to the study area. The colors indicate the Vulnerability Index values or the vulnerability levels of the regions along the Sianok Fault to earthquakes. The color scale from light green to dark red indicates vulnerability levels from low to high; light green indicates areas with a low Vulnerability Index (Low: 10.0), while dark red shows areas that are highly vulnerable with a high vulnerability Index (High: >150.0). The colors in between, such as yellow and orange, represent vulnerability levels transitioning from low to high.

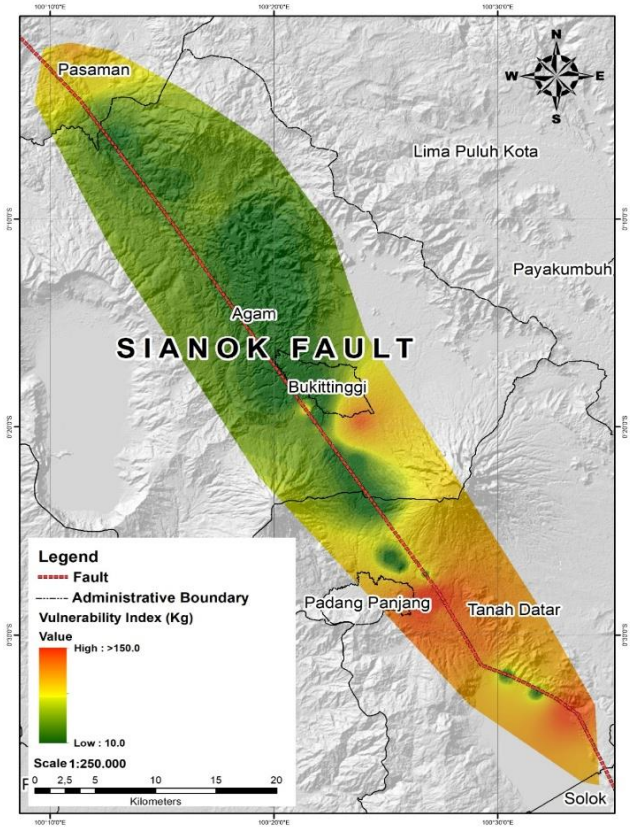

Figure 10. Map of the vulnerability index around the Sianok area Fault

The higher the value of Kg, the greater the potential for an earthquake to inflict damage on the region; conversely, the lower the value of Kg, the lesser the potential for earthquake-induced damage. The map includes part of Bukittingi in a highly vulnerable zone. This aligns with the results of the analysis, which show that Bukittinggi has softer sediments from alluvium deposits. Another area with high vulnerability is the city of Padang Panjang, which continues in the southeast towards Solok Regency.

3.4. Liquefaction Potential and Ground Shear Strain

Earthquakes will affect the soil's stability depending on the soil's nature and properties [51]. Liquefaction can occur due to the loss of effective ground tension due to cyclic loading caused by earthquake shaking [52]. Cyclic loads transmit voltage within the pores to an effective grounding tension. This phenomenon occurs when loose sandy soils are saturated with water. Consequently, the soil's ability to withstand the load is compromised, resulting in deformation [53]. When determining the liquefaction potential, higher K_g values indicate damage is more likely [54]. The Kg value comes only from the strain of the soil structure. According to SASAME [55], liquefaction can occur if the Kg value exceeds 5.0. This threshold can be defined as follows:

$$K_g = \frac{A^2}{f_0} \tag{4}$$

Figure 11 shows the liquefaction potential for the study area calculated using Equation 3 based on the HVSR results, this map shows the liquefaction potential for each area if an earthquake occurs in the future. The color scale from light green to dark red indicates the level of liquefaction potential from low to high. The light green color indicates areas with low liquefaction potential (Low: <5), while the dark red color indicates a very high liquefaction potential (High: >5). The colors in between, such as yellow and orange, represent levels of liquefaction potential that are between low and high (transition). These results provide important information, including reference information for vulnerability maps and information that can be used to design earthquake disaster prevention measures around the Sianok Fault.

The ground shear strain on the soil layer delineates the capacity of the soil material to undergo deformation or displacement during an earthquake. The ground shear strain is denoted by γ. The higher the ground shear strain value, the greater the vulnerability of the soil to deformation phenomena such as landslides and liquefaction. The ground shear strain value is determined using the subsequent equation [37]:

$$\gamma = K_g \times \alpha_b \times 10^{-6} \quad (5)$$

K_g represents the seismic vulnerability index, whereas α_b denotes the maximum ground acceleration (gals). According to the Indonesian National Standardization Agency (2019), the maximum ground acceleration value for the Sianok Fault region is 0.6 g or 588.40 gals. The relationship between ground shear strain and soil behaviour reactions, as outlined in Seht & Wohlenberg [56], is presented in Table 2.

Table 2. Soil strain based on soil dynamic properties

Size of strain γ	Phenomena	Dynamic Properties
10^{-6}	Wave	Elasticity
10^{-4}	Vibration	Elasticity
10^{-3}	Crack	Elasto-plasticity
10^{-2}	Settlement	Elasto-plasticity
10^{-1}	Landslide, liquefaction	Collapse

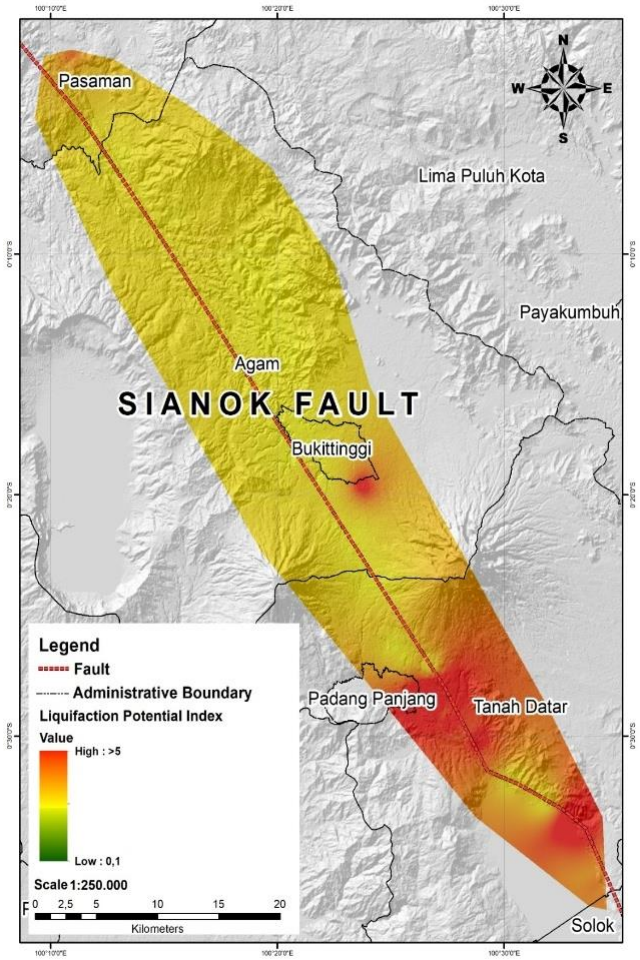

Figure 11. Liquefaction potential map of the area around the Sianok Fault

The results of the ground shear strain mapping for the study area are shown in Figure 12. Based on the Sianok Fault shear strain results obtained using Equation 3, with the maximum soil acceleration set to 0.6 g (applied predicted future maximum peak ground motion acceleration), the entire Sianok Fault area has the potential to experience soil stretching, which results in cracking, settlement, landslides, and liquefaction. This aligns with the predictions of the liquefaction potential shown in Figure 11 and calculated using Equation 4; most of the Sianok Fault area can be threatened with liquefaction. The obtained result is quite similar to liquefaction events in some places along the Sianok segment due to the Sianok segment earthquake, which had a magnitude of 6.2 on March 6th, 2007 [57].

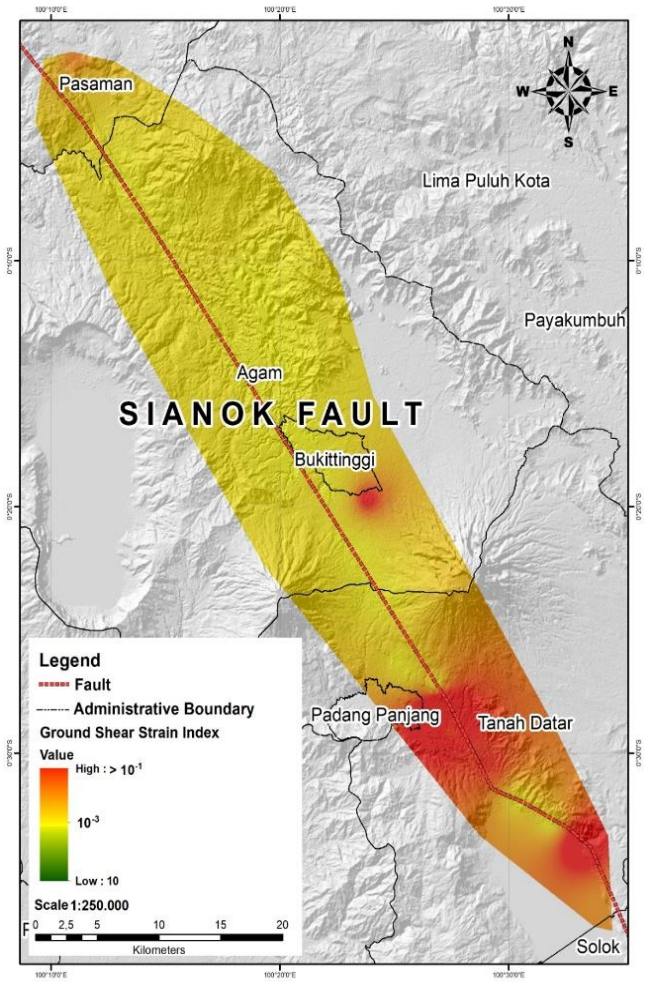

Figure 12. Ground shear strain map for the Sianok Fault based on PGA Standard Design Indonesia (0.6 g)

To ascertain the dynamic properties associated with the absence of site response and the dynamic response of the structure, two fundamental parameters were examined: the horizontal-to-vertical spectrum ratio and the floor spectrum ratio (FSR), from the microtremor single observation result [58, 59]. Microtremor single observation results are used to identify the sediment layer thickness in some cities in west Sumatera Province [60]. Cone Penetration Tests (CPT) are a methodological approach commonly employed to ascertain the engineering properties of soils [61].

This study proposes and provides complete information on disaster potential along the Sianok segment, We obtained shear velocity by considering the frequency of the subsoil structure from microtremor single observation result and its depth from field soil investigation results (cone penetration test) to obtain shear velocity for subsoil structure [62, 63] soil. The vulnerability index (Kg) serves as a critical parameter in quantifying seismic susceptibility, thereby facilitating the assessment of surface layer propensity for deformation under seismic stress. Nakamura [35] and Mittal et al. [51], the Liquefaction occurs when the Kg is greater than 5 [64-66]. The Kg multiplied with predicted ground motion acceleration can produce the strain and stress of subsoil structures [54]. covering the areas of Pasaman, Padang, Padang Panjang, Tanah Datar, and Solok—are classified as soft soil, with shear wave velocity (Vs) < 150 m/s and a natural period < 1 s. These findings are consistent with the results obtained using methods inferred from magnetic and gravity modelling [5].

We only used microtremor single observation and field soil survey cone penetration test results to determine subsoil characteristics, natural period, vulnerability index, liquefaction and stress-strain along the Sianok segment. The results show clear information on each potential for preparing mitigation by local government society along the Sianok Segment.

4. Conclusion

This study revealed the characteristics of faults and mapped the level of seismic vulnerability and the liquefaction potential of the Sianok Fault area. The site characteristics in the fault region show that the predominant period is in the range of 0.14–5.12 s. The seismic vulnerability index for the Sianok Fault varies depending on the soil's natural frequency and the rock site's amplification. The areas with high vulnerability are Bukittinggi and the city of Padang Panjang; this high vulnerability continues in the southeast direction towards Solok Regency.

As for the liquefaction potential, the seismic vulnerability index results and shear strain levels in the study area suggest that, on average, this area has the potential to experience cracking ($\gamma > 10^{-3}$) and moderate liquefaction. If a large earthquake (0.6 g) occurs there in the future, liquefaction with greater intensity is predicted in the southeastern area of the flat land district towards Solok District.

These findings offer essential insights for constructing shaking maps, updating hazard maps, and formulating disaster prevention measures in certain regions along the Sianok fault. The seismic vulnerability, soil characteristic and liquefaction susceptibility map developed in this study should not be viewed solely as a scientific product but as a spatial decision-support instrument for urban planning and infrastructure resilience in West Sumatra. Local governments are encouraged to integrate the results into regional spatial planning (RTRW), building permit procedures, and hazard mitigation strategies. High-susceptibility zones, particularly in alluvial and basin areas, should require mandatory geotechnical verification and ground improvement measures prior to development. By incorporating geophysical-based susceptibility assessment into early-stage planning, municipalities can reduce future seismic losses and promote risk-informed urban growth.

5. Declarations

5.1. Author Contributions

Conceptualization, R.R.P., J.K., and Z.Z.; methodology, R.R.P. and J.K.; software, M.D.A. and D.S.; validation, S.V., J.K., and Z.Z.; formal analysis, N.S.; investigation, T.A., F.R., A.B.P., and Z.A.; writing—original draft preparation, R.R.P.; writing—review and editing, R.R.P., J.K., Z.Z., and. S.V. All authors have read and agreed to the published version of the manuscript.

5.2. Data Availability Statement

The data presented in this study are available on request from the corresponding author.

5.3. Funding and Acknowledgments

The research described in this paper was financially supported by Universitas Negeri Padang under the Kerjasama Luar Negeri scheme (PNBP and WCU) for 2022–2023 and the Penelitian Dasar Perguruan Tinggi scheme for 2022 and 2025, under contract numbers 1212/UN35.13/KP/2022 and 492/UN35/LT/2023. The authors would like to thank Prof. Yusuke Ono from Tottori University, Japan, for his contribution to reviewing the manuscript and providing ideas for the conducted research.

The authors would also like to thank Universitas Negeri Padang for providing financial support toward the APC of this article, funded by the EQUITY Kemdiktisaintek Program supported by LPDP, under contract numbers 4310/B3/DT.03.08/2025 and 2692/UN35/KS/2025.

5.4. Conflicts of Interest

The authors declare no conflict of interest.

6. References

[1] Ansal, A., Kurtuluş, A., & Tönük, G. (2010). Seismic microzonation and earthquake damage scenarios for urban areas. Soil Dynamics and Earthquake Engineering, 30(11), 1319–1328. doi:10.1016/j.soildyn.2010.06.004.

[2] Bradley, K. E., Feng, L., Hill, E. M., Natawidjaja, D. H., & Sieh, K. (2017). Implications of the diffuse deformation of the Indian Ocean lithosphere for slip partitioning of oblique plate convergence in Sumatra. Journal of Geophysical Research: Solid Earth, 122(1), 572–591. doi:10.1002/2016JB013549.

[3] Campo, B., Bruno, L., & Amorosi, A. (2023). Sedimentary facies characterization through CPTU profiles: An effective tool for subsurface investigation of modern alluvial and coastal plains. Sedimentology, 70(4), 1302–1327. doi:10.1111/sed.13079.

[4] Cooley, J. W., Lewis, P. A. W., & Welch, P. D. (1969). The Fast Fourier Transform and its Applications. IEEE Transactions on Education, 12(1), 27–34. doi:10.1109/TE.1969.4320436.

[5] Dahrin, D., Amir, H., Suryanata, P. B., Bijaksana, S., Fajar, S. J., Ibrahim, K., Harlianti, U., Arisbaya, I., Pebrian, M. Q., Rahman, A. A., & Kasendri, A. (2022). Subsurface structures of Sianok Segment in the GSF (Great Sumatran Fault) inferred from magnetic and gravity modeling. Frontiers in Earth Science, 10. doi:10.3389/feart.2022.1012286.

[6] Damayanti, C. (2023). Analysis of Microtremor Data for Identification of Sediment Layer Thickness Based on Ground Profile Vs in Solok City, West Sumatera. Indonesian Journal of Applied Physics, 13(2), 158. doi:10.13057/ijap.v13i2.42609.

[7] Gosar, A. (2017). Study on the applicability of the microtremor HVSR method to support seismic microzonation in the town of Idrija (W Slovenia). Natural Hazards and Earth System Sciences, 17(6), 925–937. doi:10.5194/nhess-17-925-2017.

[8] Djuri, M., Samodra, H., Amin, T. C., & Gafoer, S. (1996). Geological Map of the Padang Sheet, Sumatra. Geological Research and Development Centre, Bandung, Indonesia.

[9] Bellier, O., & Sébrier, M. (1994). Relationship between tectonism and volcanism along the Great Sumatran Fault Zone deduced by spot image analyses. Tectonophysics, 233(3-4), 215–231. doi:10.1016/0040-1951(94)90242-9.

[10] Natawidjaja, D. H., Sieh, K., Ward, S. N., Cheng, H., Edwards, R. L., Galetzka, J., & Suwargadi, B. W. (2004). Paleogeodetic records of seismic and aseismic subduction from central Sumatran microatolls, Indonesia. Journal of Geophysical Research: Solid Earth, 109(B4), 1-34. doi:10.1029/2003jb002398.

[11] Sieh, K., & Natawidjaja, D. (2000). Neotectonics of the Sumatran fault, Indonesia. Journal of Geophysical Research: Solid Earth, 105(B12), 28295–28326. doi:10.1029/2000jb900120.

[12] Petersen, M. D., Dewey, J., Hartzell, S., Mueller, C., Harmsen, S., Frankel, A., & Rukstales, K. (2004). Probabilistic seismic hazard analysis for Sumatra, Indonesia and across the Southern Malaysian Peninsula. Tectonophysics, 390(1-4), 141-158. doi:10.1016/j.tecto.2004.03.026.

[13] BMKG. (2023). Earthquake Information: Bukittinggi. Badan Meteorologi, Klimatologi, dan Geofisika (BMKG), Jakarta, Indonesia. Available online: https://www.bmkg.go.id (accessed on May 2026). (In Indonesian).

[14] SNI 1726:2019. (2019). Earthquake resistance planning procedures for building and non-building structures. Badan Standardisasi Nasional (BSN), Jakarta, Indonesia. (In Indonesian).

[15] Irsyam, M., Cummins, P. R., Asrurifak, M., Faizal, L., Natawidjaja, D. H., Widiyantoro, S., ... & Syahbana, A. J. (2020). Development of the 2017 national seismic hazard maps of Indonesia. Earthquake Spectra, 36(1_SUPPL), 112-136. doi:10.1177/8755293020951206.

[16] Bard, P. Y. (1999). Microtremor measurements: a tool for site effect estimation. The effects of surface geology on seismic motion, 3, 1251-1279, Balkema, Rotterdam, Netherlands.

[17] Havenith, H. B. (2004). Guidelines for the implementation of the H/V spectral ratio technique on ambient vibrations measurements, processing and interpretation. European Commission–EVG1-CT-2000-00026 SESAME, Université de Liège, Liège, Belgium.

[18] Putra, R. R., Kiyono, J., & Ono, Y. (2012). Shaking characteristic of Padang City, Indonesia. Proceedings of the 15th World Conference on Earthquake Engineering, Lisbon, Portugal.

[19] Thein, P. S., Pramumijoyo, S., Brotopuspito, K. S., Wilopo, W., Kiyono, J., & Setianto, A. (2013). Site response characteristics of H/V spectrum by microtremor single station observations at Palu City, Indonesia. Journal of Southeast Asian Applied Geology, 5(1), 1-9.

[20] Fitri Yulianto, G., Saimima Wakano, Q., Widi Santoso, E., Ridwan, M., & Santoso, B. (2025). Preliminary study site characterization using HVSR microtremor in West Bandung Basin. E3S Web of Conferences, 604, 14001. doi:10.1051/e3sconf/202560414001.

[21] Prabowo, S. B., Wulandari, R., Putri, I. A., Nathania, E. Y., Nugraha, P., & Sitio, Y. Y. C. (2025). Assessment of Seismic Vulnerability and Shear Wave Velocity Estimation Using the Horizontal-to-Vertical Spectral Ratio (HVSR) Method in Umbul Niti Geothermal Manifestations, Jatimulyo Village, South Lampung. IOP Conference Series: Earth and Environmental Science, 1458(1), 012024. doi:10.1088/1755-1315/1458/1/012024.

[22] Robertson, P. K. (2010). Evaluation of Flow Liquefaction and Liquefied Strength Using the Cone Penetration Test. Journal of Geotechnical and Geoenvironmental Engineering, 136(6), 842–853. doi:10.1061/(asce)gt.1943-5606.0000286.

[23] Lunne, T., Powell, J. J. M., & Robertson, P. K. (2002). Cone Penetration Testing in Geotechnical Practice. CRC Press, London, United Kingdom. doi:10.1201/9781482295047.

[24] Parolai, S., Picozzi, M., Richwalski, S. M., & Milkereit, C. (2005). Joint inversion of phase velocity dispersion and H/V ratio curves from seismic noise recordings using a genetic algorithm, considering higher modes. Geophysical Research Letters, 32(1), 1-4. doi:10.1029/2004GL021115.

[25] Arai, H., & Tokimatsu, K. (2004). S-wave velocity profiling by inversion of microtremor H/V spectrum. Bulletin of the Seismological Society of America, 94(1), 53–63. doi:10.1785/0120030028.

[26] Setiawan, B., Juellyan, J., Al-huda, N., Yulianur, A., Saidi, T., & Jaksa, M. B. (2024). Sub-surface shear wave velocity models developed based on a combined in-situ measurement of quasi-static cone penetration test (q-CPT) and microtremor datasets. Data in Brief, 54, 110501. doi:10.1016/j.dib.2024.110501.

[27] Zaenudin, A., Farduwin, A., Boy Darmawan, G. I., & Karyanto. (2024). Shear wave velocity model using HVSR inversion beneath Bandar Lampung City. Earthquake Science, 37(4), 337–351. doi:10.1016/j.eqs.2024.04.004.

[28] Prasetya, A. R., Faris, F., & Rahardjo, A. P. (2024). Seismic Vulnerability Assessment Using the HVSR Method At Yogyakarta International Airport Underpass, Indonesia. International Journal of GEOMATE, 26(114), 25–33. doi:10.21660/2024.114.4082.

[29] Susilo, A., Zulaikah, S., Fauzi, A., Ilham, Ma'muri, Wirawan, K., Haniyyah, S., Zarkoni, A., Persada, Y. D., Bery, A. A., & Rouf Hasan, M. F. (2026). Seismic site characterization of Malang Regency (Indonesia) using HVSR inversion. Kuwait Journal of Science, 53(1), 100486. doi:10.1016/j.kjs.2025.100486.

[30] Amelia, R., Imran, A. M., & Sultan. (2025). Analysis of Horizontal to Vertical Spectral Ratio (HVSR) Microtremors in Quaternary Sediment Area, Takalar Regency, South Sulawesi Indonesia. IOP Conference Series: Earth and Environmental Science, 1451(1), 12042. doi:10.1088/1755-1315/1451/1/012042.

[31] Marjiyono, Setiadi, I., & Setiawan, J. (2021, October). The Estimation of Seismic Site Amplification of Bukittinggi City, West Sumatera, Indonesia. IOP Conference Series: Earth and Environmental Science, 873(1), 012009. doi:10.1088/1755-1315/873/1/012009.

[32] Liu, H. S., Zheng, T., Qi, W. H., & Lan, J. Y. (2010). Relationship between shear wave velocity and depth of conventional soils. Yantu Gongcheng Xuebao/Chinese Journal of Geotechnical Engineering, 32(7), 1142–1149.

[33] Molnar, S., Cassidy, J. F., Castellaro, S., Cornou, C., Crow, H., Hunter, J. A., Matsushima, S., Sánchez-Sesma, F. J., & Yong, A. (2018). Application of Microtremor Horizontal-to-Vertical Spectral Ratio (MHVSR) Analysis for Site Characterization: State of the Art. Surveys in Geophysics, 39(4), 613–631. doi:10.1007/s10712-018-9464-4.

[34] Mucciarelli, M. (1998). Reliability and applicability of Nakamura's technique using microtremors: An experimental approach. Journal of Earthquake Engineering, 2(4), 625–638. doi:10.1080/13632469809350337.

[35] Nakamura, Y. (1989). A Method for Dynamic Characteristics of Surface. Quarterly Report of RTRI, 30(1), Railway Technical Research Institute, Tokyo, Japan.

[36] Nakamura, N. (2005). A practical method for estimating dynamic soil stiffness on surface of multi- layered soil. Earthquake engineering & structural dynamics, 34(11), 1391-1406. doi:10.1002/eqe.487.

[37] Nakamura, Y. (1997). Seismic vulnerability indices for ground and structures using microtremor. World congress on railway research, 16-19 November, 1997, Florence, Italy.

[38] Nakamura, Y. (2000). Clear identification of fundamental idea of Nakamura's technique and its applications. Proceedings of the 12th world conference on earthquake engineering, 30 January-4 February, 2000, Auckland, New Zealand.

[39] Nakamura, Y. (2009). Basic structure of QTS (HVSR) and examples of applications. In Increasing seismic safety by combining engineering technologies and seismological data. Springer, Dordrecht, Germany.

[40] Natawidjaja, D. H. (2018). Major Bifurcations, Slip Rates, and A Creeping Segment of Sumatran Fault Zone in Tarutung-Sarulla-Sipirok-Padangsidempuan, Central Sumatra, Indonesia. Indonesian Journal on Geoscience, 5(2), 137–160. doi:10.17014/IJOG.5.2.137-160.

[41] Natawidjaja, D. H., & Triyoso, W. (2007). the Sumatran Fault Zone — From Source To Hazard. Journal of Earthquake and Tsunami, 01(01), 21–47. doi:10.1142/s1793431107000031.

[42] Olimat, W. E. (2019). Seismic site effect estimation using microtremor studies in the archaeological city of Jerash in Jordan. Acta Geologica Sinica (English Edition), 93(S1), 270. doi:10.1111/1755-6724.14081.

[43] Parolai, S., Bormann, P., & Milkereit, C. (2002). New relationships between Vs, thickness of sediments, and resonance frequency calculated by the H/V ratio of seismic noise for the cologne area (Germany). Bulletin of the Seismological Society of America, 92(6), 2521–2527. doi:10.1785/0120010248.

[44] Pornsopin, P., Pananont, P., Furlong, K. P., Chaila, S., Promsuk, C., Kamjudpai, C., & Phetkongsakul, K. (2024). Seismic Microzonation Map of Chiang Mai Basin, Thailand. Trends in Sciences, 21(3), 7370. doi:10.48048/tis.2024.7370.

[45] Prabowo, U. N., Amalia, A. F., & Budhi, W. (2019). Peak Ground Acceleration and Earthquake Intensity Microzonation in Watukumpul, Pemalang Regency. Indonesian Journal of Science and Education, 3(2), 60. doi:10.31002/ijose.v3i2.1169.

[46] Putra, R. R., Kiyono, J., Ono, Y., & Parajuli, H. R. (2012). Seismic Hazard Analysis for Indonesia. Journal of Natural Disaster Science, 33(2), 59–70. doi:10.2328/jnds.33.59.

[47] Putra, R. R., Kiyono, J., Yoshimoto, Y., Ono, Y., & Syahril. (2016). Determined soil characteristic of Palu in Indonesia by using microtremor observation. International Journal of GEOMATE, 10(2), 1737–1742. doi:10.21660/2016.20150802.

[48] Putra, R. R., Novriadi, Iskandar, G., Yandra, M., & Andayono, T. (2022). Seismic Microzonation and Liquefaction Potential Study by Using Microtremor Result Data in and Around Sipora Island, Indonesia. Civil Engineering and Architecture, 10(3), 888–898. doi:10.13189/cea.2022.100311.

[49] Kiyono, J., & Ono, Y. (2011). Estimation of earthquake ground motion in Padang, Indonesia. GEOMATE Journal, 1(1), 71-77.

[50] Rezaei, S., & Choobbasti, A. J. (2014). Liquefaction assessment using microtremor measurement, conventional method and artificial neural network (Case study: Babol, Iran). Frontiers of Structural and Civil Engineering, 8(3), 292–307. doi:10.1007/s11709-014-0256-8.

[51] Mittal, H., Wu, Y. M., Chen, D. Y., & Chao, W. A. (2016). Stochastic finite modeling of ground motion for March 5, 2012, Mw 4.6 earthquake and scenario greater magnitude earthquake in the proximity of Delhi. Natural Hazards, 82(2), 1123-1146. doi:10.1007/s11069-016-2236-x.

[52] Rong, M., Fu, L. Y., & Li, X. (2017). On the amplitude discrepancy of HVSR and site amplification from strong-motion observations. Bulletin of the Seismological Society of America, 107(6), 2873–2884. doi:10.1785/0120170118.

[53] Sakhakarmi, D., Kawan, C. K., Prajapati, A., Pradhananga, C., Karanjit, S., & Bijukchhen, S. M. (2024). Seismic microzonation and soil-structure resonance analysis in Suryabinayak Municipality, Bhaktapur, Nepal: insights from ambient vibration measurements. Geomatics, Natural Hazards and Risk, 15(1), 2311892. doi:10.1080/19475705.2024.2311892.

[54] Salamah, U. (2020). Uji Getaran Seismik Pada Rancang Bangun Real Time Seismic Measurement (Rsam) Menggunakan Fast Fourier Transform (Fft). Navigation Physics: Journal of Physics Education, 2(1), 21–24. doi:10.30998/npjpe.v2i1.272. (In Indonesian).

[55] SASAME. (2004). Guidlines for the Implementation of the H/V Spectral Ratio Technique on Ambient Vibrations. European Research Project: Vol. D23.12, European Commission, Brussels, Belgium.

[56] Seht, M. I. Von, & Wohlenberg, J. (1999). Microtremor Measurements Used to Map Thickness of Soft Sediments. Bulletin of the Seismological Society of America, 89(1), 250–259. doi:10.1785/bssa0890010250.

[57] Siburian, B. I., Marzuki, M., & Lubis, A. M. (2024). Local site effects and seismic microzonation around Suban Area, Curup Rejang Lebong, Bengkulu deduced by ambient noise measurements. Geoenvironmental Disasters, 11(1), 5. doi:10.1186/s40677-024-00268-7.

[58] Stanko, D., Markušić, S., Gazdek, M., Sanković, V., Slukan, I., & Ivančić, I. (2019). Assessment of the seismic site amplification in the city of ivanec (NW part of Croatia) using the microtremor HVSR method and equivalent-linear site response analysis. Geosciences (Switzerland), 9(7), 312. doi:10.3390/geosciences9070312.

[59] Tunçel, A. (2021). Estimation of soil dynamic parameters by using ambient noise and scenario earthquake in Aliağa/İzmir (Western Anatolia). Arabian Journal of Geosciences, 14(3), 231. doi:10.1007/s12517-021-06653-y.

[60] Unjoh, S., Kaneko, M., Kataoka, S., Nagaya, K., & Matsuoka, K. (2012). Effect of earthquake ground motions on soil liquefaction. Soils and Foundations, 52(5), 830–841. doi:10.1016/j.sandf.2012.11.006.

[61] Wils, K., Daryono, M. R., Praet, N., Santoso, A. B., Dianto, A., Schmidt, S., Vervoort, M., Huang, J. J. S., Kusmanto, E., Suandhi, P., Natawidjaja, D. H., & De Batist, M. (2021). The sediments of Lake Singkarak and Lake Maninjau in West Sumatra reveal their earthquake, volcanic and rainfall history. Sedimentary Geology, 416. doi:10.1016/j.sedgeo.2021.105863.

[62] Wulandari, B. R., & Hurukawa, N. (2013). Relocation of large earthquakes along the Sumatran fault and their fault planes. Bulletin of the International Institute of Seismology and Earthquake Engineering, 47, 25-30.

[63] Xu, R., & Wang, L. (2021). The horizontal-to-vertical spectral ratio and its applications. Eurasip Journal on Advances in Signal Processing, 2021(1), 75. doi:10.1186/s13634-021-00765-z.

[64] Yamanaka, H., Takemura, M., Ishida, H., & Niwa, M. (1994). Characteristics of long-period microtremors and their applicability in exploration of deep sedimentary layers. Bulletin - Seismological Society of America, 84(6), 1831–1841. doi:10.1785/bssa0840061831.

[65] Yan, P., Li, Z., Li, F., Yang, Y., Hao, W., & Bao, F. (2018). Antarctic ice sheet thickness estimation using the horizontal-to-vertical spectral ratio method with single-station seismic ambient noise. Cryosphere, 12(2), 795–810. doi:10.5194/tc-12-795-2018.

[66] Zheng, M., Huang, Y. M., Liang, J. W., He, S. Y., Li, X. D., Chen, H. W., Su, B., Su, X. M., & Xie, C. (2024). Correlation Analysis of Shear Wave Velocity and Burial Depth in Rock and Soil in the Yulin Area. Earthquake, 44(1), 78–93. doi:10.12196/j.issn.1000-3274.2024.01.006.